Proceedings paper

Scand J Work Environ Health 1995;21(2):22-26

Direct interaction between crystalline silica and DNA -- a proposed model for silica carcinogenesis

by Daniel LN, Mao Y, Williams AO, Saffiotti U

Key terms: carcinogenesis mechanisms; deoxyribonucleic acid; DNA; DNA binding; electron microscopy; FRLE cell line; infrared spectra; quartz

This article in PubMed: www.ncbi.nlm.nih.gov/pubmed/8929683

Scand J Work Environ Health 1995;21 suppl 2:22—6

Direct interaction between crystalline silica and DNA – a proposed model for silica carcinogenesis

by Lambert N Daniel, MD,[1] Yan Mao, PhD,[1] A Olufemi Williams, MD,[1] Umberto Saffiotti, MD[1]

Daniel LN, Mao Y, Williams AO, Saffiotti U. Direct interaction between crystalline silica and DNA — a proposed model for silica carcinogenesis. *Scand J Work Environ Health* 1995;21 suppl 2:22—6.

Crystalline silica in aqueous buffer produced oxygen radicals that mediated in vitro DNA (deoxyribonucleic acid) strand breakage. The oxidized DNA base, thymine glycol, was also produced. The hydroxyl radical, responsible for most DNA damage, has a reaction distance of about 15 Angstroms, requiring close contact of silica with DNA. Fourier transform infrared spectroscopy of incubations of quartz particles with DNA showed distinct alterations in both DNA and quartz spectra and therefore indicated extensive hydrogen bonding between surface silanol groups and the phosphate-sugar backbone of DNA. Electron microscopy and energy dispersive X-ray spectroscopy of alveolar epithelial cells in fetal rat lung, exposed to quartz in culture, showed localization of quartz particles in the nuclei and mitotic spindles. Direct interaction of crystalline silica with DNA may be important in silica carcinogenesis by anchoring DNA close to sites of free radical production on the silica surface, or by interfering with DNA replication, repair, or the mitotic process.

Key terms carcinogenesis mechanisms, deoxyribonucleic acid, DNA binding, FRLE cell line, electron microscopy, infrared spectra, quartz.

Human exposure to crystalline silica particles causes silicosis (1). Many studies show an increased risk for lung cancer associated with silicosis (2—5). The carcinogenic activity of quartz in vivo has been well established by numerous studies in rats (3, 6—13). In vitro models have also been developed for crystalline silica toxicity (14, 15) and neoplastic cell transformation (16, 17). The physicochemical basis of these effects has not been established, however.

Properties of crystalline silica that have been proposed to account for its pathogenicity include the hydrogen bonding ability of surface silanol groups (18), the negative surface charge produced by ionized surface silanol groups (14), and the generation of oxygen-free radicals at the silica surface (15, 19—22). Crystalline silica produces damage of DNA (deoxyribonucleic acid) in vitro (19, 20), a mechanism which could be involved in its ability to induce neoplastic cell transformation and carcinogenic effects in vivo. However, the hydroxyl radical mediating this type of DNA damage has a reaction distance of approximately 15 Angstroms (23), less than the width of a DNA helix. Adhesion of DNA to amorphous silica, such as glass and silica gel, is well known (24). DNA binding to crystalline silica might also be expected, and this binding could be important in anchoring DNA close to sites of free radical production at the surface of crystalline silica particles. In order to investigate the mechanisms of silica carcinogenicity through direct DNA damage, we addressed the following major questions: (i) what is the mechanism of DNA binding to quartz and (ii) is quartz able to interact with nuclear material in the alveolar epithelial cells — the cell of origin for silica-induced lung carcinomas?

Materials and methods

Silica preparations. A sample of Min-U-Sil 5 α-quartz (MQZ) from the Pittsburgh Glass and Sand Co (now US Silica, Berkeley Springs, West Virginia, United States) was obtained in 1984 through the Illinois Institute of Technology Research Institute (19, 25). Chinese standard α-quartz (CSQZ) (26) was obtained from the Institute of Occupational Medicine, Chinese Academy of Preventive Medicine, Beijing, China. Both samples were characterized for surface area and binding to Janus Green B (25).

The quartz samples were dried in an oven at 110°C for 24 h prior to each experiment, suspended in buffer at 20 mg · ml^{-1} and sonicated for 3 min in a sonicator bath (Branson model 220, Shelton, Connecticut, United States). The suspensions were diluted to the desired concentrations and used immediately to ensure homogeneity.

DNA and chemicals. Calf thymus DNA and chemical reagents were obtained from Sigma (St Louis, Missouri, United States). Phosphate buffers were treated with Chelex resin (Biorad, Richmond, California, United States) and titrated to pH 7.4 by mixing monovalent and divalent stock solutions. One molar stock buffers were diluted to 5 mM by adding H_2O or D_2O. Titration of buffers containing heavy water (D_2O) to pD 7.4 was obtained by adding the value of 0.45 to the pH meter reading (27).

1 Laboratory of Experimental Pathology, National Cancer Institute, Bethesda, Maryland, United States.

Reprint requests to: Dr U Saffiotti, Laboratory of Experimental Pathology, National Cancer Institute, Building 41, Room C-105, Bethesda, Maryland 20892—0041, USA.

Fourier transform infrared spectroscopy. The attenuated total reflectance (ATR) Fourier transform infrared (FT-IR) spectroscopic methods used were based on previously published procedures (28, 29). A single-beam FTS-45 FT-IR spectrophotometer (Biorad, Cambridge, Massachusetts, United States) was used with a DTGS detector to obtain spectra (resolution 8 cm^{-1}) at ambient temperatures. For each sample, 1000 scans were taken. The samples were scanned in a liquid ATR cell (Biorad) using a zinc selenide (45°) crystal. Spectral analysis was limited to the range of 1800 to 800 cm^{-1}. All the ATR spectra were recorded under nitrogen atmosphere to minimize water vapor interference. Vibrational signals arising from buffer components were subtracted from sample spectra according to standard subtraction criteria (30, 31). The effects of DNA-silica coincubation were observed by subtracting recorded spectra for DNA or silica from the combination spectrum. In order to obtain correct silica subtraction, distinct silica peaks at 779 and 799 cm^{-1} were used as an internal normalization standard. The criterion for DNA subtraction was a flat base line in the 1750 to 1200 cm^{-1} range (29).

Transmission FT-IR spectra were obtained in a standard fluid cell between parallel zinc selenide windows (Perkin-Elmer, Norwalk, Connecticut, United States).

Cell culture and electron microscopy. The FRLE cell line, derived from fetal rat lung alveolar type II cells (32) (which correspond to the cell of origin for silica-induced rat lung adenocarcinoma) was kindly provided by Dr MA Haralson, Department of Pathology, Vanderbilt University School of Medicine, Nashville, Tennessee, United States, and further characterized in our laboratory (33). Cells at passage 39° were plated at 10^4 cells per 50-mm dish in minimal essential medium (MEM) with 10% fetal bovine serum. At 24 h after the plating the medium was changed to an aliquot containing MQZ or CSQZ (dispersed by sonication immediately before the treatment) at a final concentration of 25 $\mu g \cdot cm^{-2}$. For the electron microscopy, the cultures at 2, 8, and 26 d after silica exposure were washed, fixed in situ with 1.5% glutaraldehyde, postfixed in 1% osmium tetroxide, stained with uranyl acetate, and embedded in pure epoxy resin (LX-112). Thin sections were cut with diamond knives parallel and perpendicular to the cell monolayer. The thin sections were mounted on a formvar film grid and double stained with uranyl acetate and lead citrate. Sections were examined and photographed with a Hitachi H-7000 electron microscope at 100 kV.

Energy dispersive X-ray analysis. Kevex-ray energy dispersive X-ray (EDX) analysis was made in the STEM (scanning transmission electron microscopy) mode on a Hitachi H-7100 microscope operated at 75 kV (TEM mode) and 10 kV (SEM mode). A 68° X-ray takeoff angle detector was used for the silica particle analysis.

Results

Infrared spectroscopy. With the use of transmission FT-IR, consistent peaks were recognizable for DNA (10 $mg \cdot ml^{-1}$) in phosphate buffer (figure 1A) and for quartz in suspension (5 $mg \cdot ml^{-1}$) (figure 1B). MQZ showed a major peak at 1088 cm^{-1} with a prominent shoulder peak at 1163 cm^{-1}. Corresponding peaks were seen at 1095 cm^{-1} and 1161 cm^{-1} for CSQZ (29). Combination spectra obtained by quartz-DNA coincubation produced tracings dominated by the quartz spectrum at the concentrations used. These tracings were characterized by a narrowing of the major peak for quartz and a shift of approximately 9 cm^{-1} (figure 1C). These findings are consistent with a loss of degeneracy in the spectrum due to silicon-oxygen bond alteration on the surface of the silica crystal, presumably as a result of DNA binding to the silanol group.

ATR infrared spectroscopy was performed using 10 $mg \cdot ml^{-1}$ DNA in phosphate buffer, combined with 0.2, 1.0, or 5.0 $mg \cdot ml^{-1}$. The lower silica doses were used in order to increase the ratio of DNA to silica in the combination spectra, which had been dominated by silica in the transmission spectra. DNA spectra were obtained which agreed with previously published spectra (28, 34, 35) (figure 2, dotted lines). When DNA was coincubated with MQZ, the subtraction spectrum [(DNA+quartz)-quartz] showed a major shift in the region of 1053 cm^{-1} of the DNA spectrum (figure 2, upper panel). Both MQZ and CSQZ produced

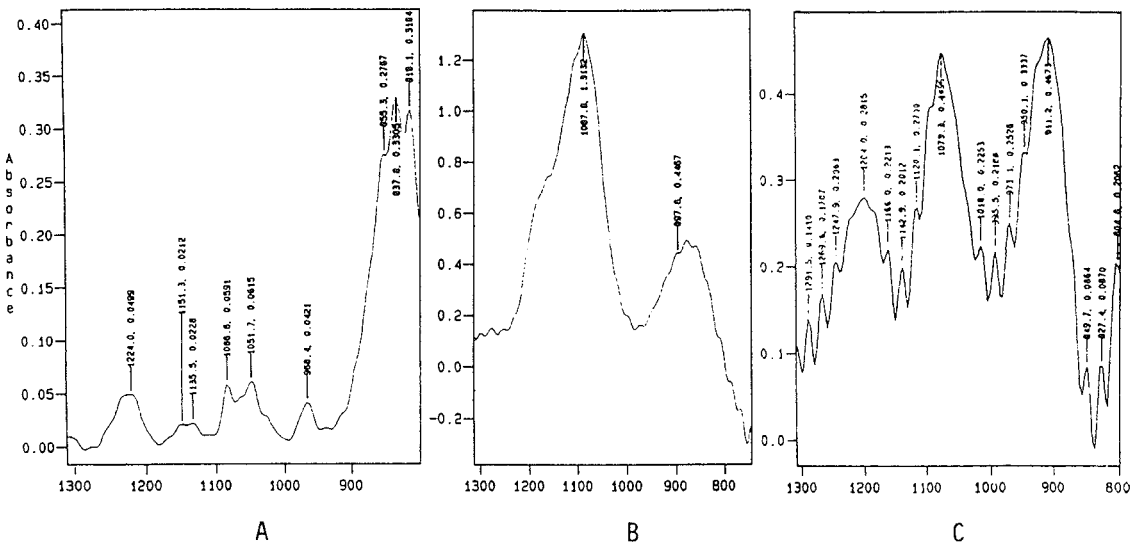

Figure 1. Transmission FT-IR spectra in the region near 1000 cm^{-1}: A = DNA 10 $mg \cdot ml^{-1}$, B = MQZ quartz (5 $mg \cdot ml^{-1}$ suspension), C = DNA plus MQZ. Note the splitting of the broad major peak of MQZ at 1088 cm^{-1} into two narrower peaks at 1204 and 1079 cm^{-1}. The peak at 911 cm^{-1}, which appears to be new, cannot be identified due to strong water absorbance in this region. (Note the different scales of the panels).

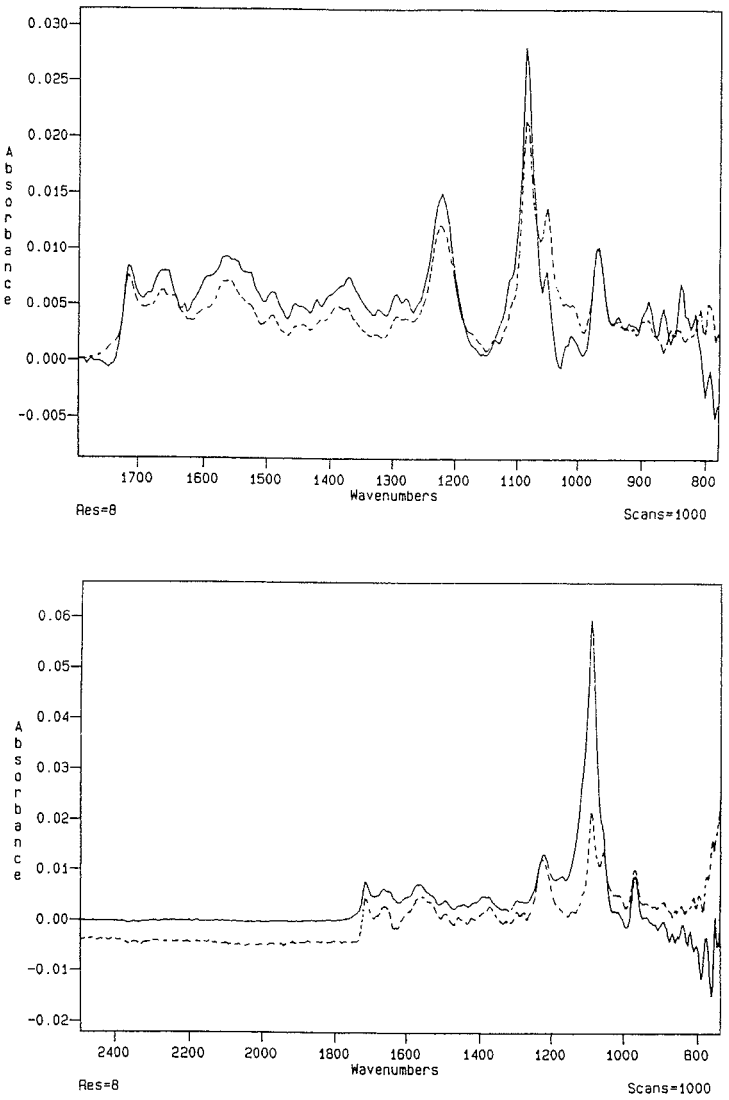

Figure 2. ATR infrared spectra: upper panel = DNA plus MQZ quartz, lower panel = DNA plus CSQZ quartz. Note the different scales of the panels. (----- = DNA alone, ——— = DNA plus quartz after subtraction of the quartz spectrum)

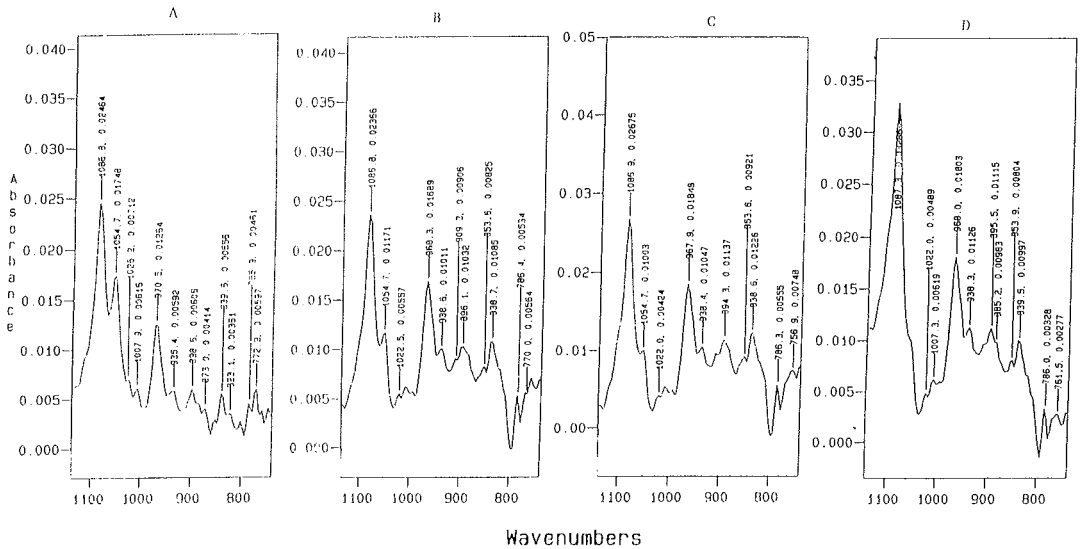

Figure 3. ATR infrared spectra in D_2O: A = DNA (10 mg · ml^{-1}), B = DNA + 0.2 mg · ml^{-1} MQZ quartz, C = DNA + 1 mg · ml^{-1} MQZ, D = DNA + 5 mg · ml^{-1} MQZ. The subtraction factor for normalization is 1.025. (Note the different scales of the Y axes).

marked alterations in the ratios of the peaks at 1086 and 1053 cm^{-1} (figure 2). These peaks correspond, respectively, to symmetric stretching of the PO_2^- in the sugar phosphate backbone of DNA and to either the phosphodiester or the C-O stretch of the sugar ring (28). Since the region below 1000 cm^{-1} could not be accurately measured due to water absorbance, spectra were obtained using D_20 (figure 3). The spectrum for DNA alone (A) was compared with the subtraction spectra obtained from DNA mixed with increasing amounts of MQZ (B,C,D). The effect of increasing amounts of MQZ on the DNA spectrum is evident, with a marked increase in the height of the peak at 1086 cm^{-1} and a progressive loss of the shoulder at 1053 cm^{-1}. Smaller but significant changes were noted in the 1800 to 1500 cm^{-1} region of the DNA spectrum (29). Band alterations observed at 1688 cm^{-1} may indicate a perturbation of the planar base stacking caused by subtle conformational changes in the DNA helix or by bending of the DNA duplex as it wraps around bound silica particles (29).

Electron microscopy and energy dispersive X-ray analysis. A thorough search by electron microscopy for silica particles in the nuclei of FRLE cells, exposed to quartz in culture, revealed that some cells contained small (< 0.5 μm) particles inside the nuclei (figure 4). The intranuclear particles were confirmed as silica by EDX spectrometry (not shown). Quartz particles were also sought in cells undergoing mitosis and were found in mitotic spindles, although not in intrachromatinic locations.

Discussion

Vibrations arising from different parts of the DNA macromolecule correspond to infrared absorptions detectable in different parts of the spectrum (35). The changes in infrared spectra described in this presentation are consistent with an interaction of silica at the phosphate backbone of the DNA molecule. The finding that silica-DNA binding occurs at the phosphate backbone suggests that the proximity of the DNA to the particle surface may be important in the induction of strand breaks by silica through hydroxyl radicals (29). The finding that CSQZ produced more marked effects on the DNA spectrum than MQZ is consistent with the greater surface area of CSQZ (25). The role of the silanol groups on the quartz surface in the DNA binding interaction is supported by evidence obtained by pretreating quartz with poly(2-vinylpyridine-*N*-oxide (PVPNO), a polymer that binds to silanol groups. PVPNO-pretreated quartz did not induce modification of the ATR-FT-IR spectrum of DNA (29).

We propose a model for quartz carcinogenesis, based on the interaction of quartz particles with DNA. Our present and previous results (29) indicate that quartz particles bind DNA in vitro by hydrogen bonding of the DNA backbone to surface silanol groups. DNA damage, induced in vitro by crystalline silica, was found to be mediated by the formation of oxygen radicals on the silica surface (19). The finding of small quartz particles in the nuclei and mitotic spindles of alveolar epithelial cells exposed in culture suggests that a direct contact of quartz and nuclear material is possible in living cells and may occur in vivo. We propose that the binding of crystalline silica to cellular DNA may produce DNA damage in vivo, by anchoring DNA within a few Angstroms of the sites of oxygen-free radical production on the silica surface. This anchoring mechanism enables short-lived toxic radicals, such as the hydroxyl radical, to reach DNA bases and induce DNA damage, which becomes critical for mutagenesis, neoplastic cell transformation, and carcinogenesis. The binding of crystalline

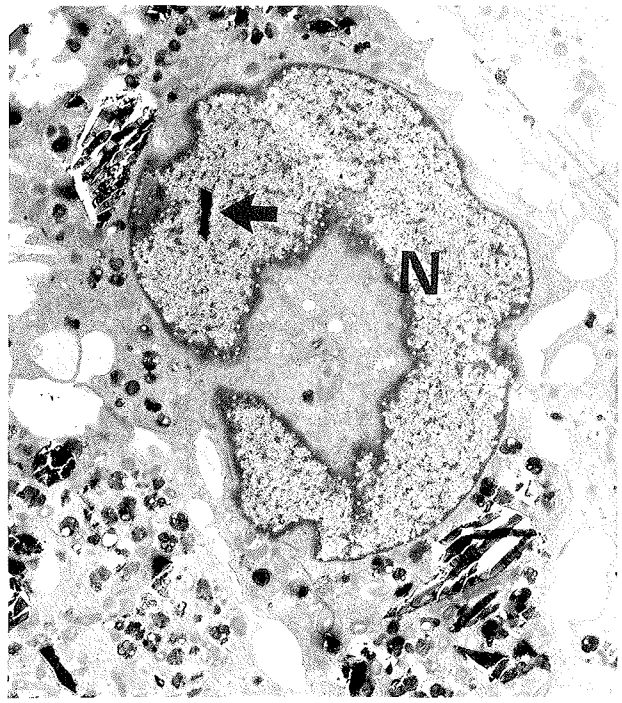

Figure 4. Intranuclear quartz particle (arrow) in a nucleus from FRLE cells exposed to 25 μg · m^{-2} MQZ quartz and sectioned after 26 d. Note two aggregates of silica particles in the cytoplasm of the cell. Energy dispersive X-ray spectroscopic analysis of the intranuclear quartz particle revealed distinct silica peaks (not shown).

silica to DNA may also lead to DNA damage by interfering with the replication, repair, or expression of DNA or by altering the mitotic process.

The mutagenicity of crystalline silica needs to be studied in appropriate systems. Hei et al (36) have demonstrated the mutagenic activity of asbestos fibers (crocidolite and chrysotile) using a target cell system capable of detecting large multilocus deletions. Similar studies with silica have not yet been conducted. Recent studies by Driscoll et al (37) showed that rat lung epithelial cells, harvested from F344 rats 15 months after the instillation of crystalline silica at three different dose levels, had mutation frequencies for the *hprt* gene that were markedly increased in a dose-dependent manner, up to more than 20 times the frequency for untreated controls. The evidence that quartz induced neoplastic transformation and chromosome aberrations in cells in culture (16, 17) further supports the hypothesis that crystalline silica is capable of producing DNA damage in living cells. We do not know how crystalline silica particles come in contact with DNA in vivo, in spite of chromatin packaging. Preferential interaction at sites of DNA unwinding during transcription is a possible hypothesis requiring further investigation.

Acknowledgments

The authors wish to thank Ira W Levin and Noel F Whittaker for their advice in the infrared spectrometry studies.

References

1. Ziskind M, Jones RN, Weill H. Silicosis: state of the art. Am Rev Respir Dis 1976;113:643—65.
2. Goldsmith DF, Winn DM, Shy CM, editors. Silica, silicosis and cancer. New York (NY): Praeger, 1986.

3. International Agency for Research on Cancer (IARC). Silica. In: IARC. Silica and some silicates. Lyon: IARC, 1987:92—93. IARC monographs on the evaluation of the carcinogenic risk of chemicals to humans, vol 42.
4. Simonato L, Fletcher AC, Saracci R, Thomas TL, editors. Occupational exposure to silica and cancer risk. Lyon: International Agency for Research on Cancer (IARC), 1990. IARC scientific publications, no 97.
5. Western Consortium for Public Health. Second international symposium on silica, silicosis and cancer: program syllabus. Berkeley, CA: Western Consortium for Public Health, 1993.
6. Groth DH, Stettler LE, Platek SF, Lal JB, Burg JR. Lung tumors in rats treated with quartz by intratracheal instillation. In: Goldsmith DF, Winn DM, Shy CM, editors. Silica, silicosis and cancer. New York (NY): Praeger, 1986:243—53.
7. Dagle GE, Wehner AP, Clark ML, Buschbom RL. Chronic inhalation exposure of rats to quartz. In: Goldsmith DF, Winn DM, Shy CM, editors. Silica, silicosis and cancer. New York (NY): Praeger, 1986:255—66.
8. Holland LM, Wilson JS, Tillery MI, Smith DM. Lung cancer in rats exposed to fibrogenic dusts. In: Goldsmith DF, Winn DM, Shy CM, editors. Silica, silicosis and cancer. New York (NY): Praeger, 1986:267—79.
9. Johnson NF, Smith DM, Sebring R, Holland LM. Silica-induced alveolar cell tumors in rats. Am J Ind Med 1987;11:93—107.
10. Muhle H, Takenaka S, Mohr U, Dasenbrock C, Mermelstein R. Lung tumor induction upon long-term low-level inhalation of crystalline silica. Am J Ind Med 1989;15:343—6.
11. Spiethoff A, Wesch H, Wegener K, Klimisch H-J. The effects of thorothrast and quartz on the induction of lung tumors in rats. Health Phys 1992; 63:101—10.
12. Saffiotti U. Lung cancer induction by crystalline silica. Prog Clin Biol Res 1992;374:51—69.
13. Saffiotti U, Daniel LN, Mao Y, Williams AO, Kaighn ME, Ahmed N, et al. Biological studies on the carcinogenic mechanisms of quartz. Rev Mineral 1993;28:523—44.
14. Nolan RP, Langer AM, Harrington JS, Oster G, Selikoff IJ. Quartz hemolysis as related to its surface functionalities. Environ Res 1981;26:503—20.
15. Vallyathan V, Shi X, Dalal NS, Irr W, Castranova V. Generation of free radicals from freshly fractured silica dust. Am Rev Respir Dis 1988; 138:1213—9.
16. Hesterberg TW, Barrett JC. Dependence of asbestos and mineral dust-induced transformation of mammalian cells in culture on fiber dimension. Cancer Res 1984;44:2170—80.
17. Saffiotti U, Ahmed N. Neoplastic transformation by quartz in the BALB/3T3/A31-1-1 cell line and the effects of associated minerals. Teratogenisis Carcinogenisis Mutagenesis. In press.
18. Nash T, Allison AC, Harrington JS. Physicochemical properties of silica in relation to its toxicity. Nature 1966;210:259—61.
19. Daniel LN, Mao Y, Saffiotti U. Oxidative DNA damage by crystalline silica. Free Radic Biol Med 1993;14:463—72.
20. Shi X, Mao Y, Daniel LN, Saffiotti U, Dalal NS, Vallyathan V. Silica-radical-induced DNA damage and lipid peroxidation. Environ Health Perspect 1994;102 suppl 10:159—63.
21. Fubini B, Bolis V, Giamello E, Pugliese L, Volante M. The formation of oxygen reactive radicals at the surface of the crushed quartz dusts as a possible cause of silica pathogenicity. In: Mossman BT, Bégin RO, editors. Effects of mineral dusts on cells. Berlin: Springer-Verlag, 1989:205—14.
22. Doelman CJA, Leurs R, Oosterom, WC, Bast A. Mineral dust exposure and free radical mediated lung damage. Exp Lung Res 1990;16:41—55.
23. Meneghini R. Genotoxicity of active oxygen species in mammalian cells. Mutat Res 1988;195:215—30.
24. Boom R, Sol CJA, Salimans MMM, Jansen CL, Wertheim-van-Dillen PME, van der Noordaa J. Rapid and simple method for purification of nucleic acids. J Clin Microbiol 1990;28:495—503.
25. Daniel LN, Mao Y, Vallyathan V, Saffiotti U. Binding of the cationic dye, Janus Green B, as a measure of the specific surface area of crystalline silica in aqueous suspension. Toxicol Appl Pharmacol 1993;123:62—7.
26. Fu SC, Yang GC, Shong MZ, Du QZ. Characterization of a new standard quartz and its effects in animals [in Chinese]. Chin J Ind Hyg Occup Dis 1984;2:134—7.
27. Covington AR, Paabo M, Robinson RA, Bates RG. Use of the glass electrode in deuterium oxide and the relation between the standardized pD (paD) scale and the operational pH in heavy water. Anal Chem 1968;40:700—6.
28. Dev SB, Walters L. Fourier transform infrared spectroscopy for the characterization of a model peptide-DNA interaction. Biopolymers 1990;29:289—99.
29. Mao Y, Daniel LN, Whittaker N, Saffiotti U. DNA binding to crystalline silica characterized by Fourier-transform infrared spectroscopy. Environ Health Perspect 1994;102 suppl 10:165—71.
30. Dev SB, Keller J, Rha CK. Secondary structure of 11S globulin in aqueous solution investigated by FT-IR derivative spectroscopy. Biochem Biophys Acta 1988;957:272—80.
31. Mohr SC, Sokolov NVHA, He C, Setlow P. Binding of small acid-soluble spore proteins from Bacillus subtilis changes the conformation of DNA from B to A. Proc Natl Acad Sci USA 1991;88:77—81.
32. Leheup BP, Federspiel SJ, Guerry-Force ML, Wetherall NT, Commers PA, DiMari SJ, et al. Extracellular matrix biosynthesis by cultured fetal rat lung epithelial cells: I. characterization of the clone and the major genetic types of collagen produced. Lab Invest 1989;60:791—807.
33. Saffiotti U, Kaighn ME, Knapton AD, Williams AO. Transformation of the fetal rat alveolar type II cell line, FRLE, by lipofection with a mutated K-ras gene [abstract]. Proc Am Assoc Cancer Res 1993;34:102.
34. Theophanides T. Fourier transform infrared spectra of calf thymus DNA and its reactions with the anticancer drug cisplatin. Appl Spectrosc 1981;35:461—465.
35. Taillandier E, Liquier J. Infrared spectroscopy of DNA. Methods Enzymol 1992;211:307—35.
36. Hei TK, Piao CQ, He ZY, Vannais D, Waldren CA. Chrysotile fiber is a strong mutagen in mammalian cells. Cancer Res 1992;52:6305—9.
37. Driscoll KE, Carter JM, Howard BW, Hassenbein DG. An in vivo model to investigate the mutagenicity of mineral dust exposure for rat lung epithelial cells [abstract]. FASEB J 1994;8:A805.